



HAL
open science

Effects of cadmium, inorganic mercury and methyl-mercury on the physiology and metabolomic profiles of shoots of the macrophyte *Elodea nuttallii*

Claudia Cosio, D Renault

► **To cite this version:**

Claudia Cosio, D Renault. Effects of cadmium, inorganic mercury and methyl-mercury on the physiology and metabolomic profiles of shoots of the macrophyte *Elodea nuttallii*. *Environmental Pollution*, 2020, 257, pp.113557. 10.1016/j.envpol.2019.113557 . hal-02393954

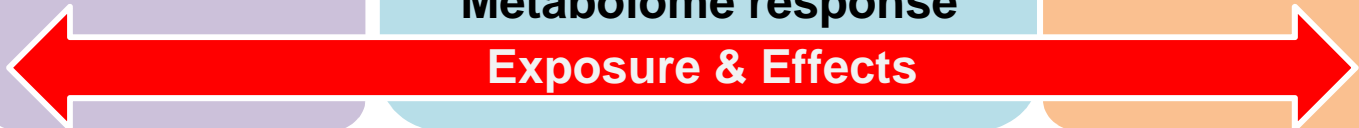
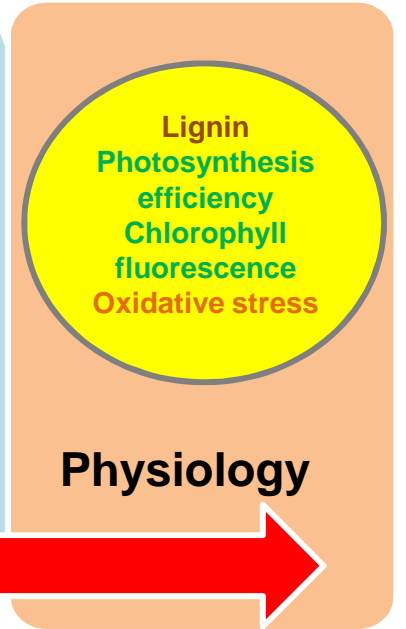
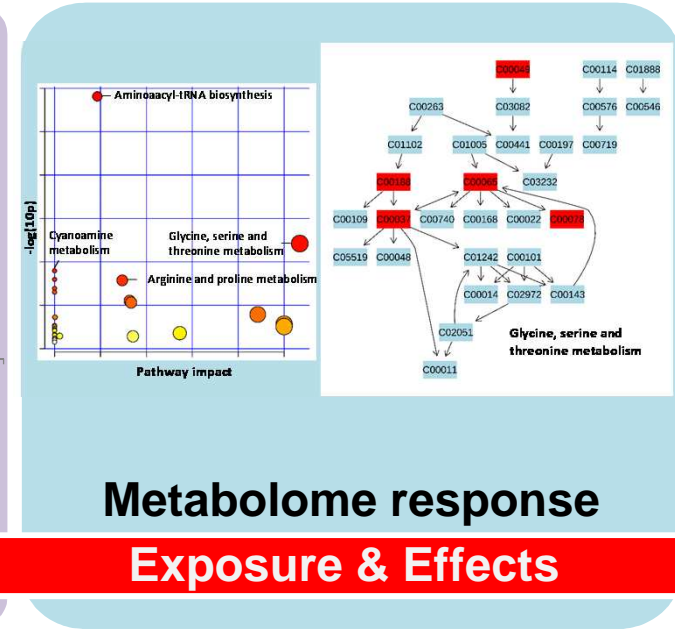
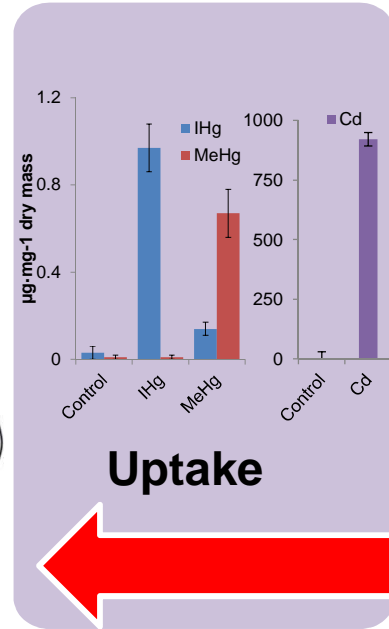
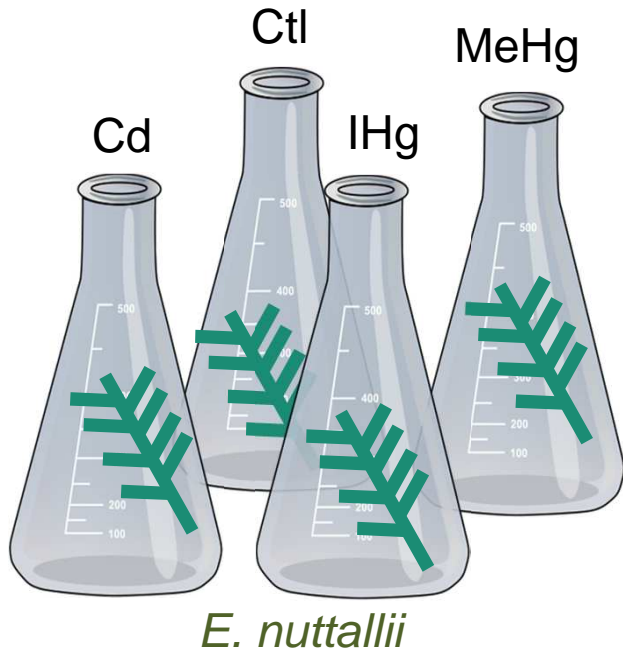
HAL Id: hal-02393954

<https://univ-rennes.hal.science/hal-02393954>

Submitted on 3 Feb 2020

HAL is a multi-disciplinary open access archive for the deposit and dissemination of scientific research documents, whether they are published or not. The documents may come from teaching and research institutions in France or abroad, or from public or private research centers.

L'archive ouverte pluridisciplinaire **HAL**, est destinée au dépôt et à la diffusion de documents scientifiques de niveau recherche, publiés ou non, émanant des établissements d'enseignement et de recherche français ou étrangers, des laboratoires publics ou privés.



1 **Effects of cadmium, inorganic mercury and methyl-mercury on the physiology and metabolomic**
2 **profiles of shoots of the macrophyte *Elodea nuttallii***

3

4 Claudia Cosio^{1,*} and David Renault^{2,3}

5

6 ¹ Université de Reims Champagne Ardennes, UMR-I 02 INERIS-URCA-ULH SEBIO, F-51687 Reims,
7 France

8 ² Université de Rennes 1, UMR 6553 EcoBio CNRS, F-35042 Rennes, France

9 ³ Institut Universitaire de France, 1 rue Descartes, 75231 Paris CEDEX 05, France

10

11

12 *Corresponding author: claudia.cosio@univ-reims.fr

Journal Pre-proof

13 **ABSTRACT**

14 Macrophytes are known to bioaccumulate metals, but a thorough understanding of tolerance
15 strategies and molecular impact of metals in aquatic plants is still lacking. The present study aimed
16 to compare Hg and Cd effects in a representative macrophyte, *Elodea nuttallii* using physiological
17 endpoints and metabolite profiles in shoots and cytosol.

18 Exposure 24h to methyl-Hg ($23 \text{ ng}\cdot\text{L}^{-1}$), inorganic Hg ($70 \text{ ng}\cdot\text{L}^{-1}$) and Cd ($281 \text{ }\mu\text{g}\cdot\text{L}^{-1}$) did not affect
19 photosynthesis, or antioxidant enzymes despite the significant accumulation of metals, confirming a
20 sublethal stress level. In shoots, Cd resulted in a higher level of regulation of metabolites than MeHg,
21 while MeHg resulted in the largest number of regulated metabolites and IHg treatment regulated no
22 metabolites significantly. In cytosol, Cd regulated more metabolites than IHg and only arginine,
23 histidine and mannose were reduced by MeHg exposure. Kyoto Encyclopedia of Genes and Genomes
24 (KEGG) pathway analysis of data suggested that exposure to MeHg resulted in biochemical changes
25 including aminoacyl-tRNA biosynthesis, glycine, serine and threonine metabolism, nitrogen
26 metabolism, arginine and proline metabolism, cyanoamino acid metabolism, while the treatment of
27 Cd stress caused significant variations in aminoacyl-tRNA biosynthesis and branched-chain amino
28 acids pathways. Data supports an impact of MeHg on N homeostasis, while Cd resulted in an osmotic
29 stress-like pattern and IHg had a low impact. Marked differences in the responses to MeHg and IHg
30 exposure were evidenced, supporting different molecular toxicity pathways and main impact of
31 MeHg on non-soluble compartment, while main impact of IHg was on soluble compartment.
32 Metabolomics was used for the first time in this species and proved to be very useful to confirm and
33 complement recent knowledge gained by transcriptomics and proteomics, highlighting the high
34 interest of multi-omics approaches to identify early impact of environmental pollution.

35

36 **Keywords:** amino acids, cytosol, macrophyte, shoots, sugars.

37

38 **Capsule:** Metabolomics reveal different cellular toxicity responses to sublethal Cd, MeHg and IHg
39 treatment in *Elodea nuttallii*

40

41 1. INTRODUCTION

42 Anthropogenic activities result in environmental contamination by mercury (Hg) and cadmium (Cd)
43 (Loizeau et al., 2013; Azimi and Rocher, 2016). As a result, biota is affected by the toxicity of these
44 toxic metals, which can also affect human populations *via* contaminated food (Croteau et al., 2005;
45 Bravo et al., 2010; Niane et al., 2014). Metals can enter the food chain through primary producers,
46 including macrophytes, which represent a key group within communities of shallow water, in terms
47 of biomass, primary production, food source and shelter for fauna. Importantly, macrophytes are
48 also central to oxygen, pollutants and nutrients biogeochemical cycles (Wetzel, 2001; Chambers et
49 al., 2008; Bonanno and Lo Giudice, 2010; Noges et al., 2010). High levels of Cd, inorganic Hg (IHg)
50 and methyl-Hg (MeHg) can be observed in aquatic ecosystems colonized by plants (Samecka-
51 Cymerman and Kempers, 2003; Castro et al., 2009; Regier et al., 2013b). Therefore, bioaccumulation
52 of metals in macrophytes represents a significant and current environmental concern (Beauvais-
53 Fluck et al., 2016; Beauvais-Fluck et al., 2017).

54 Due to their ability to accumulate and tolerate high concentrations of metals (Regier et al., 2013b;
55 Cosio et al., 2014), aquatic plants are often seen as good candidates for phytoremediation,
56 biomonitoring and ecotoxicology investigations (Valega et al., 2009; Bonanno and Lo Giudice, 2010;
57 Cosio et al., 2014). However, physiological mechanisms associated with metal accumulation and
58 prevention of their toxicity are still poorly understood in those plants, preventing the full
59 optimization of their use for environmental applications. Increasing the knowledge on the biology
60 and physiology of these plants, and more particularly the impact of metal accumulation on their
61 metabolism is therefore a research priority (Cosio et al., 2014).

62 *Elodea nuttallii* is a macrophyte widely distributed in temperate regions, and it is well-known for its
63 accumulative capacity of metals (Larras et al., 2013; Regier et al., 2013b). Several recent studies used
64 transcriptomics and proteomics approaches to describe cellular toxicity of Cd and Hg in *E. nuttallii*,
65 with the aim of using this plant for active biomonitoring. Data revealed rapid molecular changes in
66 metal-exposed plants (Larras et al., 2013; Regier et al., 2013a; Regier et al., 2013b; Regier et al.,
67 2016; Beauvais-Fluck et al., 2018a; Beauvais-Fluck et al., 2018b). These studies, spanning a wide
68 range of concentrations, globally suggest toxic metals to impact genes and proteins involved in cell
69 structure (lignin content), energy metabolism (sugar and photosynthesis), amino acid metabolism,
70 and to trigger anti-oxidative stress responses (Larras et al., 2013; Regier et al., 2013a; Regier et al.,
71 2013b; Regier et al., 2016; Beauvais-Fluck et al., 2018b). Besides, several differences were observed
72 between IHg and MeHg responses. At the transcriptome level, MeHg deregulated more genes than
73 IHg at similar intracellular concentrations (Beauvais-Fluck et al., 2018b). At the proteome level, 200
74 $\text{ng}\cdot\text{L}^{-1}$ IHg had a significant and similar effect than $500 \mu\text{g}\cdot\text{L}^{-1}$ Cd exposure, while $30 \text{ng}\cdot\text{L}^{-1}$ MeHg was

75 similar to controls, showing non-significant changes in proteome (Larras et al., 2013). Data thus
76 suggest different cellular toxicity pathways for IHg and MeHg. However, for both transcriptomic and
77 proteomic, many regulated contigs or peptides had an unknown function indicating considerable
78 potential for new discoveries in the biology of toxic metals.

79 Views obtained from transcriptomics, proteomics and physiological studies depict distinct levels of
80 regulation that exist in the organism. Transcriptomic informs on the level of expression of genes, but
81 cellular functions of a particular gene are carried out by its protein. Regulation of proteins in turn
82 results in alterations in levels of small metabolites involved in biochemical reactions in the functional
83 organism. Gene regulation might happen to maintain protein levels, whereas changes in the
84 abundance of proteins can be related to posttranslational modifications of proteins. Eventually,
85 proteins carry out a myriad of functions within the cell, including the metabolism of small molecules
86 such as amino acids and sugars, known to have functional roles in plant abiotic stress tolerance and
87 signaling (Yancey, 2005). Physiological adjustments and degradation of pollutants is thus ultimately
88 sustained by the metabolic network, whose production of energy, and primary and secondary
89 metabolites, are central for physiological repair and remodeling of cells. In this context,
90 metabolomics enables a large physiological representation of the effect of pollutants by incorporating
91 metabolic fluxes, enzymatic kinetics, and the resulting action of the stressors at organismal level.
92 Metabolic reconfigurations in plants exposed to pollutants, and more generally to a range of abiotic
93 stressors, result in the up-regulation and down-regulation of specific metabolic functions to sustain
94 biological functions (sustainers) and control/modulate metabolite fluxes (modulators) (Topfer et al.,
95 2014; Tohge et al., 2015).

96 In this context, metabolomics give the opportunity to confirm or reveal effects of toxicants in a way
97 that cannot be fully exploited by other molecular approaches (*e.g.* proteomics and transcriptomics).

98 In the present study, we analyzed the metabolic profiles of cytosol and shoots in *E. nuttallii* exposed
99 to Cd, IHg or MeHg, and their control counterparts, to obtain a comprehensive phenotyping of the
100 effects of sublethal concentrations of these toxicants. Metal uptake and physiological endpoints
101 were also measured. We hypothesized that amino acids and sugars should be associated with the
102 high tolerance of *E. nuttallii* to toxic metals, and thus, should be measured in higher amounts in
103 metal-exposed plants.

104

105 **2. EXPERIMENTAL SECTION**

106 **2.1. Lab-ware and reagents**

107 All laboratory material was soaked in 10% v/v HNO₃ (*pro analysis*, Merck, Nyon, Switzerland)
108 followed by two 10% v/v HCl (*pro analysis*, Merck, Nyon, Switzerland) acid baths for ≥ 1 week,

109 thoroughly rinsed with ultrapure water (<18.2 M Ω , MilliQ Direct system, Merck Millipore,
110 Darmstadt, Germany) and dried under a laminar flow hood. MeHg (CH₃HgCl) standard solution (1 g·L⁻¹)
111 ¹) was obtained from Alfa Aesar (Ward Hill, MA, USA), while IHg (Hg(NO₃)₂) and Cd (Cd(NO₃)₂)
112 standard solutions (1 g·L⁻¹) were obtained from Sigma-Aldrich (Buchs, Switzerland).

113

114 **2.2. Plant culture and exposure to toxic metals**

115 Shoots of *Elodea nuttallii* (Planch.) St. John were collected in Lake Geneva (Switzerland, N46° 16'
116 28.7" E6° 10' 15.7"), and a culture was established and maintained in microcosms as previously
117 described (Regier et al., 2013b). Cultures and experiments were conducted in the laboratory under
118 controlled conditions (20 °C, 16/8 h with 5.84 W m⁻² photosynthetically active radiation [PAR], 1000
119 lux, 20 ± 1 °C). We exposed (or not: control) for 24h in triplicate three 10 cm-long shoots without
120 roots in 1L bechers filled with 1.2 μ m filtered Lake Geneva water spiked with 30 ng·L⁻¹ MeHg
121 (nominal concentration 30 ng·L⁻¹, effective concentration 23 ± 7 ng·L⁻¹ MeHg), 70 ng·L⁻¹ IHg (nominal
122 concentration 200 ng·L⁻¹, effective concentration 70 ± 14 ng·L⁻¹ IHg) or 280 μ g·L⁻¹ Cd (nominal
123 concentration 500 μ g·L⁻¹, effective concentration 281 ± 24 μ g·L⁻¹ Cd).

124

125 **2.3. Hg and Cd uptake**

126 After the 24h-long exposure to toxic metals, shoots were rinsed with 1 mM EDTA for IHg or Cd
127 treatments, and with 1 mM EDTA + 1 mM cysteine for MeHg treatments, to assess intracellular
128 metal concentrations (*i.e.* not extractable portion) (Larras et al., 2013).

129 For total Hg (THg = IHg + MeHg), lyophilized shoots of *E. nuttallii* were analyzed by AMA-254. For
130 MeHg, shoots were ground, freeze-dried, and extracted by HNO₃ leaching/CH₂Cl₂ extraction. Then,
131 they were analyzed by ethylation onto Tenax traps, followed by GC separation and cold vapor atomic
132 fluorescence spectrometry (GC-CV-AFS), as described in Liu et al. (2012). For Cd, shoots were
133 ground, freeze-dried and analyzed by ICP-MS (HP 4500, Agilent) after mineralization into 4 mL HNO₃
134 *s.p.* and 1 mL H₂O₂ *s.p.*

135 THg and Cd in cytosol (see cytosol extraction protocol below) were measured by cold vapor atomic
136 fluorescence spectroscopy (CV-AFS, 2500 Tekran) and ICP-MS, respectively. MeHg in cytosol was
137 measured by the hydride generation method with cryogenic trapping, gas chromatography and
138 atomic fluorescence spectrometry (CT-GC-AFS) (Stoichev et al., 2004).

139 For all metal analysis methods, the analytical quality was assured by analyzing certified reference
140 material, blanks and several samples twice.

141

142 **2.4. Physiological endpoints**

143 Chlorophyll content was measured by spectrophotometry (Cosio and Dunand, 2010). Chlorophyll
144 fluorescence allows determining PSII efficiency, and was measured using a Handy PEA fluorimeter
145 (Hansatech Instruments Ltd, Norfolk, UK). Plants were dark adapted for 15 min before illuminating
146 them for 1 sec while recording increase in fluorescence. The performance index PI(abs) was
147 calculated from measured fluorescence. The activities of class III peroxidases (POD) and superoxide
148 dismutases (SOD) were assessed by spectrophotometry (Cosio and Dunand, 2010; Regier et al.,
149 2016). Lignin content was measured by thyoglycolic attack (Cosio and Dunand, 2010).

150

151 **2.5. Cytosol extraction**

152 Fresh plants were prepared as described in Regier et al. (2013b). Briefly, fresh plants were all
153 collected at the same time, and weighed before being ground into 10 mL buffer (0.25M sucrose, 1
154 mM DTT, 50 mM Tris HCl pH 7.5). The resulting mixture was centrifuged at 500 g for 5 min at 4 °C.
155 Supernatant, which contained cytosol, was collected and frozen until further used for analysis of
156 metabolite concentrations. The dry mass of the whole shoots was calculated from the fresh biomass
157 of each shoot weighed before the sap extraction based on previous observations that dry mass
158 represents in average 18.3% of fresh mass for shoots.

159

160 **2.6. Analysis of metabolites**

161 For metabolomics, shoots of the plants exposed to the different experimental conditions for 24h
162 were all collected at the same time, and immediately frozen in liquid nitrogen. Shoot were kept
163 frozen at -30 °C until analysis. Three independent replicates, consisting of a pool of three shoots, or
164 corresponding to the pooled cytosols of three plants (see section 2.5 for the method used for cytosol
165 extraction), were run for each experimental condition. The plant samples were homogenized into
166 600 µL of ice-cold (-20 °C) methanol-chloroform solution (2:1, v:v) using a tungsten-bead beating
167 apparatus (RetschTM MM301, Retsch GmbH, Haan, Germany) at 25 agitations per second for 1.5
168 min. Then, a volume of 400 µl of ice-cold ultra-pure water was added to each sample, and samples
169 were subsequently vortexed and centrifuged at 4000 g for 10 min at 4 °C. A volume of 600 µL of the
170 upper aqueous phase (which contained polar metabolites) was transferred to new microtubes, and
171 further used for GC-MS and LC assays.

172

173 *GC-MS Analyzes*

174 Sixty (cytosol) or 120 (shoots) µL of the upper aqueous phase were transferred to new glass vials,
175 and these aliquots were vacuum-dried (MiVac, Genevac Ltd., Ipswich, England) at 32 °C for 45 min.
176 Then, we used the derivatization process and GC-MS settings described in Khodayari et al., (2013).

177 Briefly, the dried aliquots were resuspended in 30 μL of 20 $\text{mg}\cdot\text{L}^{-1}$ methoxyamine hydrochloride
178 (Sigma-Aldrich, St. Louis, MO, USA) in pyridine, incubated under automatic orbital shaking at 40 °C
179 for 90 min. Subsequently, 30 μL of N-methyl-N-(trimethylsilyl) trifluoroacetamide (MSTFA; Sigma)
180 was added and the derivatization was conducted at 40 °C for 45 min under agitation. Our GC-MS
181 system consisted of a Trace GC Ultra chromatograph and a Trace DSQII quadrupole mass
182 spectrometer (Thermo Fischer Scientific, see Khodayari et al., (2013) for more details). Randomized
183 sample sequences were established for sample injection, chromatograms were deconvoluted using
184 *XCalibur* v2.0.7. Standard samples, consisting of 62 pure reference compounds at 1, 2, 5, 10, 20, 50,
185 100, 200, 500, 750, 1000, and 1500 μM were run, and metabolite levels were quantified using the
186 quadratic calibration curves for each reference compound.

187

188 *LC analyzes*

189 Amino acid analysis was adapted from Renault et al. (2010) and (2016). Briefly, 100 μL of the
190 metabolites in solution in the methanol-ultra-pure water extract was vacuum-dried (MiVac, Genevac
191 Ltd., Ipswich, England) at 32 °C for 30 min, and the pellet was re-suspended into 100 μL of ultra-
192 pure water. Then, aliquots (10 μL) of the aqueous extracts were used for amino acids derivatization
193 according to the AccQ•Tag ultra derivatization kit protocol (Waters Corporation, Milford, MA).
194 Amino acids were analyzed using an Acquity UPLC®533 system (Waters Corporation, Milford, MA) by
195 injecting 1 μL of the derivatization mix onto an Acquity UPLC®534 BEH C18 1.7 μm 2.1 x 100 mm
196 column heated at 55 °C. External standards were run and used for the drawing of calibration curves,
197 further allowing the quantification of the metabolites from the samples.

198

199 **2.7. Data Analysis**

200 Principal component analysis (PCA) was performed to identify patterns in response of variables and
201 individuals, and compare the responses of the plants exposed to the three metal treatments, and
202 the control. PCA were conducted with the packages FactoMineR (<http://factominer.free.fr/>) and
203 ade4 (<http://pbil.univ-lyon1.fr/ade4>) in the R software (<http://www.r-project.org>). Normality and
204 homoscedasticity were tested, and a student's t-test was used in Excel (Microsoft, Redmond, WA,
205 USA) to determine if two sets of data were significantly different. For the metabolic pathway
206 analysis, the name of compounds that exhibited significant variations were analyzed in
207 MetaboAnalyst (<http://www.metaboanalyst.ca>). The library of metabolic pathways was assembled
208 from the KEGG database, and the significance of the pathway name was assessed with the Holm-
209 Bonferroni method.

210

211 3. RESULTS

212 3.1. Bioaccumulation of metals in the plants and effects on physiological endpoints

213 The 24h-exposure of *E. nuttallii* to Cd, IHg and MeHg resulted in a significant bioaccumulation of
214 metals in shoots (Table 1). Yet, this accumulation had no significant impact on measured
215 physiological endpoints: lignin and chlorophyll contents, photosynthesis, POD and SOD activities,
216 whose values were non-significantly different from control plants (Table 1).

217

218 3.2. Metabolites in shoots

219 We investigated the impact of short sublethal exposures to Cd, IHg and MeHg on the metabolic
220 phenotypes of shoots of *E. nuttallii* (Table S1). In whole shoots, Cd treatment increased the
221 concentrations of 11 amino acids, two sugars, one polyol (adonitol) and one organic acid (pipecolic
222 acid), and reduced the amounts of two amino acids (aspartic acid, methionine), relative to
223 control plants. Most strongly up-regulated amino acids by Cd included leucine, isoleucine and
224 tryptophan showing a 16× increase, and tyrosine as well as valine showing 11× and 10× increase,
225 respectively, after 24h of exposure to metals. Aspartic acid and methionine were reduced
226 0.05× and 0.3×, respectively by the 24h exposure to Cd. Similarly, MeHg exposure increased the
227 amounts of ammonium and of 13 amino acids, and reduced the concentration of one polyol (arabitol
228 0.5×) (Table 2). Most strongly up-regulated amino acids included BABA (4×), tryptophan and
229 methionine (2×). Exposure to IHg had no significant impact on concentrations of the measured
230 metabolites in shoots, as compared with control plants.

231 Principal component analysis (PCA) was performed to compare metabolic profiles among
232 treatments: 52% of the total variance was explained on axes 1 and 2 (Figure 1A and S1). In this PCA,
233 Cd-exposed shoots showed the most distinct pattern, while centroids of IHg and MeHg-treated
234 shoots were relatively similar to controls. Axis 1 was mainly constructed by the variations of
235 adonitol, maltose, isoleucine, valine, tryptophan, tyrosine and leucine. Axis 2 was mainly supported
236 by the variations of galactonolactone, glycerol, phosphoric acid, galactose, asparagine, glucose-6-
237 phosphate and glyceric acid. In shoots, the metabolic pathway analysis performed thanks to KEGG
238 databases revealed two biological metabolic pathways regulated by Cd: aminoacyl-tRNA
239 biosynthesis, and valine, leucine and isoleucine biosynthesis. IHg had no significant impact at the
240 level of pathways, while MeHg significantly impacted five metabolic pathways: aminoacyl-tRNA
241 biosynthesis, glycine, serine and threonine metabolism, nitrogen metabolism, arginine and proline
242 metabolism, cyanoamino acid metabolism.

243

244 3.3. Metabolites in the cytosol

245 Because amino acid and sugars transfer happens at the cellular level, we also investigated the
246 impact of short sublethal exposures to Cd, IHg and MeHg on the metabolic phenotypes in the cytosol
247 of *E. nuttallii*. Many amino acids are synthesized in the chloroplast and transported into the cytosol
248 for protein and secondary metabolite synthesis, or transported and stored in the vacuole. Similarly,
249 the transport of sugars and distribution of metabolites between compartments is coordinated in
250 plants to drive growth and development. In the cytosol of plants, treatments significantly modified
251 the concentration of several metabolites (Table 3): amounts of ammonium (1.7×), glycine (2.2×),
252 hydroxyproline (1.6×) and phosphoric acid (2.2×) were increased by exposure to Cd. Concentrations
253 of alpha-alanine (0.6×), aspartic acid (0.5×), galactose (0.4×), and mannose (0.3×) were reduced in
254 Cd-exposed plants. Ammonium concentration rose by 1.6× in plants exposed to IHg, while this
255 exposure reduced the amount of arginine (0.2×). In MeHg-exposed plants, changes of the
256 concentration of individual amino acids, relative to controls, were significantly reduced for histidine
257 (completely depleted) and arginine (0.2×). Regarding sugars, mannose was also reduced by IHg
258 (0.6×) and MeHg (0.3×), and galactose by MeHg (0.3×). No significant variation was reported at the
259 level of the metabolic pathways in the cytosol of the treated plants, as compared with control
260 plants.

261 Principal component analysis of metabolites in cytosol explained 60% of the variance of samples on
262 the first and second axes (Figure 1B and S2). Plants exposed to Cd showed the most distinct
263 metabolic phenotypes relative to control plants on both axes 1 and 2. While MeHg-treated plants
264 were separated from controls on axis 2, the centroid of IHg-treated plants was close to the one of
265 their control counterparts. The first axis of the PCA was mainly supported by the variations of
266 tryptophan, valine, proline, glutamic acid, phenylalanine, GABA and threonine. The second axis was
267 constructed by the variations of glucose, galactose, mannose, alpha-alanine, inositol, aspartic acid
268 and fructose.

269

270 4. DISCUSSION

271 4.1. Bioaccumulation and physiological endpoints

272 Both bioaccumulation and physiological endpoint analyses confirmed that metal concentrations
273 used here resulted in their significant bioaccumulation, with sublethal effects for *E. nuttallii*, as
274 earlier reported in other studies (Larras et al., 2013; Regier et al., 2013b; Beauvais-Fluck et al.,
275 2018b). Chosen concentrations of metal in our work are representing a compromise between high
276 concentrations resulting in unambiguous metal accumulation pattern in macrophytes, and
277 concentrations with environmental relevance. Earlier investigations using the same concentrations
278 of Cd ($281 \mu\text{g}\cdot\text{L}^{-1}$) and IHg ($70 \text{ ng}\cdot\text{L}^{-1}$) for 7d revealed that root growth was reduced, while lignification

279 of stems was increased in *E. nuttallii* (Larras et al., 2013). Nevertheless, these treatments had no
280 effects on chlorophyll content and shoot growth (Larras et al., 2013; Regier et al., 2013b).
281 Conversely, exposure to MeHg (23 ng·L⁻¹) for 7d increased root growth, suggesting a hormesis effect
282 that is seen as an overcompensation of a moderate stress (Larras et al., 2013). Similarly in another
283 study, exposure for 2h to 10 ng·L⁻¹ or 10 µg·L⁻¹ MeHg had no significant effect on chlorophyll content,
284 POD and SOD activities in *E. nuttallii* (Beauvais-Fluck et al., 2018b). In sum, consistent with the
285 literature and based on the absence of effects of the physiological endpoints, our experimental
286 conditions did not induce an acute stress in *E. nuttallii* shoots. Eventually, these data confirmed that
287 *E. nuttallii* is highly tolerant to metals.

288

289 **4.2. Effects of metals on the metabolic phenotypes of macrophytes**

290 We were interested in obtaining a general picture of effects of toxic metals on the physiology of the
291 plants by comparing their metabolic signatures. Our metabolic profiling revealed that all treatments
292 impacted metabolite amounts in shoots, cytosol or both, as compared with control plants. The Cd-
293 treated plants were characterized by the most distinct metabolic phenotypes according to PCA, in
294 both shoots and cytosol. This finding highlights a higher impact of this metal on the amount of each
295 metabolite, as also evidenced by a higher level of regulation (up to 16×) than the one measured in
296 IHg and MeHg treatments. Even if this distinction may partially result from the higher Cd
297 concentration used as compared with IHg and MeHg, we must re-emphasize that we did not find
298 differences among the three treatments and the control for the other physiological endpoints.
299 Moreover, metabolic pathway analysis suggested that MeHg impacted more metabolic pathways in
300 shoots than did Cd in our experimental conditions. A previous proteomic study with identical
301 experimental conditions suggested similar responses, and stress-induced level of IHg and Cd in *E.*
302 *nuttallii*, and an absence of response for MeHg (Larras et al., 2013). Conversely, transcriptomic
303 analyses suggested similar stress levels for Cd and IHg and a higher molecular impact of MeHg
304 (Regier et al., 2013a; Beauvais-Fluck et al., 2018b). When examining responses of the two considered
305 compartments (shoots and cytosol), we observed that Cd and MeHg both significantly impacted
306 several pathways in shoots, while IHg had no significant impact on metabolites pathways. For
307 cytosol, Cd had a higher impact than IHg, while MeHg had lower impact than IHg. Both cytosolic
308 compartment analysis and proteomics target soluble molecules, suggesting that IHg might impact
309 mainly soluble compartments, while MeHg impacts mainly the non-soluble compartments. However,
310 these differences reflect different molecular toxicity pathways of the three metals, and highlight the
311 interest of coupling analysis at different levels of organization. Indeed, the present study brings a
312 different pattern as compared with those previously observed by transcriptomics. For instance,

313 MeHg was earlier reported as a stronger dysregulator than IHg, by affecting a much higher number
314 of genes in *E. nuttallii* (Beauvais-Fluck et al., 2018b). In our study, metabolomics confirmed that
315 MeHg has a stronger molecular effect than IHg in shoots, but not in cytosol. In addition, Cd, IHg, and
316 MeHg regulated genes involved in biosynthesis of sulfur-containing amino acids such as methionine
317 and cysteine (Regier et al., 2013a; Beauvais-Fluck et al., 2018a; Beauvais-Fluck et al., 2018b).
318 Methionine was increased 2× by MeHg in shoots supporting its role in MeHg response, while
319 cysteine was not altered after metal exposure in shoots or cytosol, suggesting that regulation at the
320 gene and protein level was mostly happening to maintain the level of this metabolite.

321

322 **4.3 Early signs of stress responses in *Elodea nuttalli* treated with Cd**

323 Exposure of *E. nuttalli* resulted in a significant re-patterning of the metabolic phenotype, with for
324 instance a significant effect on the concentrations of metabolites involved in aminoacyl-tRNA
325 biosynthesis, and on the branched-chain amino acids. Aminoacyl-tRNA biosynthesis is involved in the
326 synthesis of proteins in organisms, and are particularly central to growth (Banerjee et al., 2011;
327 Raina and Ibba, 2014). Most often, the activity of this pathway declines when plants are exposed to
328 stressful or restrictive conditions, as requirements for protein synthesis is reduced to favor the
329 activation of stress-response genes (Holcik and Sonenberg, 2005). In parallel, we also found that Cd
330 treatment impacted the concentration of branched-chain amino acids (*i.e.* leucine, isoleucine and
331 valine) in shoots of *E. nuttalli*. Branched-chain amino acids share four enzymes for their biosynthesis,
332 which are coordinately regulated. Plants that accumulate and tolerate high Cd amounts, such as
333 *Solanum nigrum*, have been demonstrated to accumulate isoleucine and valine in roots (Xu et al.,
334 2012). Branched amino acids derive from the shikimate pathway, and are required for protein
335 synthesis and production of aromatic secondary metabolites, *e.g.* flavonoids, lignin cell wall
336 components, and anthocyanins, which are important for cell wall extensibility and non-enzymatic
337 anti-oxidative response both involved in metal tolerance in plants (Tzin and Galili, 2010; Zemanova
338 et al., 2017). Branched-chain amino acids also serve as precursors for the production of secondary
339 metabolites (*e.g.* alkaloids, glycosides) involved in responses to biotic and abiotic stress (Rizhsky et
340 al., 2004). These secondary metabolites notably play a role during osmotic stress (Zemanova et al.,
341 2017). Our metabolite profiling thus suggests that Cd exposure results in an osmotic stress to *E.*
342 *nuttallii*, as depicted by the 10× to 16× increase of leucine, isoleucine and valine that typically
343 accumulate in osmotically challenged plants. This hypothesis is further supported by the significant
344 accumulation of proline, a well-known biomarker of water stress in plants. Indeed, proline can act as
345 an osmolyte, a metal chelator, an antioxidative defense molecule and a signaling molecule (Hayat et
346 al., 2012).

347 The probable osmotic stress induced by Cd-exposure likely increased the amount of oxidative stress
348 experienced by the plants. Oxidative stress has been shown to alter the activity of the Krebs cycle
349 (Obata and Fernie, 2012), with potential side effects on the pathway connected to the TCA, and thus
350 on the levels of TCA-cycle-derived compounds. This includes aspartic acid, whose levels decreased in
351 shoots (and to a lesser extent in the cytosol) of Cd-treated plants. Besides, we also measured
352 decreased amounts of mannose and galactose in shoots of *E. nuttalli*. These two sugars are involved
353 in the Smirnov-Wheeler pathway, and their reduction suggests that they were used for the
354 biosynthesis of ascorbic acid. Ascorbic acid is widely recognized as an important ROS scavenger in
355 plants, and earlier studies reported that accumulation or enhanced production of ascorbic acid
356 boosted the ability of plants to cope with salt or drought stress, by limiting the peroxidation of
357 membrane lipids and reducing losses of the chlorophyll content (Venkatesh and Park, 2014).
358 Increased ROS production in Cd-treated plant is very likely, as this is a reported toxic effect of metal
359 exposure at higher concentrations (Kieffer et al., 2009; Xu et al., 2012; Larras et al., 2013).
360 Finally, the accumulation of leucine, isoleucine and valine may serve to promote stress-induced
361 protein synthesis, and may act as signaling molecules to regulate gene expression (Joshi et al., 2010).
362 The breakdown products of these three amino acids, *e.g.* acetyl-CoA, propionyl-CoA, and
363 acetoacetate, are potential energy sources for plants (Joshi et al., 2010). The global increase of
364 numerous amino acids likely depicts increased degradation and synthesis of proteins (Vital et al.,
365 2017). Similar observation was reported in crop cultivars, and shown to be linked to impact of
366 osmotic stress on the proteasome (Vital et al., 2017).

367

368 **4.4. MeHg affects the nitrogen metabolism and triggers chemical defenses against abiotic** 369 **stress**

370 In macrophytes exposed 24h to MeHg, the amount of several amino acids, including aspartic acid,
371 glutamine, glycine, phenylalanine, proline, threonine and tryptophan were altered in shoots. This
372 finding is congruent with previous transcriptomic studies conducted on *E. nuttalli* exposed to MeHg,
373 which showed that genes involved in synthesis of proteins represented a high proportion of
374 regulated genes (Beauvais-Fluck et al., 2018a). Altogether, data suggest a rapid adjustment of the
375 plants to MeHg exposure. Several of these amino acids are expected to have a role in chemical
376 defenses against abiotic stresses, notably glycine, threonine and proline (as discussed above).
377 Our metabolomic data, and more particularly the significant rise of glutamine and ammonium
378 amounts, further support that MeHg affects nitrogen (N) metabolism and homeostasis in the plant.
379 The increase of the amount of aspartic acid and glutamine in MeHg-treated plants, and the
380 concomitant reduction of ammonium amount in cytosol, suggest that N transport is altered. In

381 plants, the main pathway of ammonia assimilation is the GS/GOGAT cycle, where glutamine
382 synthetase / glutamate synthase cooperate (Masclaux-Daubresse et al., 2006). Plants may also
383 utilize the reaction catalyzed by glutamate dehydrogenase for ammonia assimilation, especially
384 under environmental stress conditions (Masclaux-Daubresse et al., 2006). Consequently, in plants,
385 aspartic acid, asparagine, glutamic acid and glutamine are the main amino acids transporter of N
386 (Miesak and Coruzzi, 2002). Here, the increase in ammonia and glutamine (high N/C ratio) suggest
387 that nitrate assimilation is affected, and both ammonia and amino acids are released by protein
388 degradation and hydrolysis. Similarly, previous transcriptomic study in *E. nuttallii* exposed to IHg,
389 MeHg or Cd highlighted a down-regulation of genes coding for nitrate and ammonium transport (e.g.
390 high affinity nitrate transporters) suggesting a global impact of tested metals on nutrition (Regier et
391 al., 2013a; Beauvais-Fluck et al., 2018a).

392 Phenylalanine, threonine, and tryptophan are aromatic amino acids coupled with the
393 phenylpropanoid and the shikimate pathways. Phenylpropanoids are a diverse group of compounds
394 derived from the carbon skeleton of phenylalanine. These compounds are involved in plant defense
395 and generate cell wall components (e.g. lignin) and antioxidant metabolites (e.g. anthocyanin)
396 (Fraser and Chapple, 2011). In previous study, a significant increase of anthocyanin, acting as non-
397 enzymatic antioxidants (Beauvais-Fluck et al., 2018a; Beauvais-Fluck et al., 2018b), was measured in
398 *E. nuttallii* exposed 2h to $10 \text{ ng}\cdot\text{L}^{-1}$ MeHg and higher concentrations, but not after IHg treatments
399 (Beauvais-Fluck et al., 2018b). The increase amount of phenylalanine, threonine, and tryptophan
400 suggests enhanced antioxidant activity in MeHg-treated plants.

401

402 **4.5. Toxic metals had little effects on the concentration of sugars**

403 A previous study hypothesized that the accumulation of fructose, galactose, sucrose and glucose in
404 poplar (*Populus tremula* L.) exposed to Cd might act as osmoprotectants playing critical roles in
405 osmotic adjustments, and protection of cell membranes against toxic trace metals (Kieffer et al.,
406 2009). Here, exposures decreased mannose and galactose amounts in cytosol. Both sugars are
407 involved in the ascorbic acid biosynthetic pathway, a major antioxidant in higher plants, and their
408 decrease is thus in line with expected cellular toxicity of metals (Ma et al., 2014). Other studies
409 suggested cellular adjustments to control resources distribution within cells: reduced sugar
410 utilization in the presence of Cd and consequently photoassimilates partial storage as sugars (Moya
411 et al., 1995; Bailey et al., 2003). In the aquatic plant *Wolffia arrhizal*, sugar and protein contents
412 were negatively correlated with toxic metal concentrations (Piotrowska et al., 2010; Zhang et al.,
413 2017). In the same line, sugars accumulated in correlation with a decline of net photosynthetic rates
414 in rice exposed to Cd (Moya et al., 1995). Similarly, amino acid metabolism often is expected to be

415 closely related to abiotic stress tolerance (Zhang et al., 2017). However, in our study few sugars
416 varied between treated and control plants, both in cytosol and shoots. Nevertheless, we observed
417 an increase of sugars in shoots, while their content concomitantly decreased in cytosol. The
418 transport of sugars and distribution between storage, respiration and biosynthesis in sink tissues are
419 coordinated activities in plants (Rosa et al., 2009a; Lemoine et al., 2013). Stress-related increase in
420 sugar delivery to sinks is important for growth, cell turgor and water potential maintenance
421 (Lemoine et al., 2013). Besides, soluble sugars have several roles in cells, including as metabolic
422 resources, structural constituents of cells, but also in stress signaling (Rosa et al., 2009b).
423 Transporters are required for efficient movement of sugars that are polar solutes across membranes
424 (Patrick et al., 2013). It is likely that multiple sugar transporters operate for fine-tuning of sugar
425 fluxes for homeostasis and interaction with other proteins for sugar sensing and signaling, including
426 efficient unloading into cell wall spaces, uptake of sucrose or transport via the apoplasm. However,
427 metal exposure concentrations used here might be too low to impact significantly sugar metabolic
428 pathways. Metabolic data thus support that previously observed regulation of genes and proteins
429 involved in sugar metabolism was mostly happening to maintain the level of those metabolites
430 (Regier et al., 2013a; Beauvais-Fluck et al., 2018a; Beauvais-Fluck et al., 2018b).

431

432 5. CONCLUSION

433 Metabolomic analysis showed that exposure of *E. nuttallii* to Cd, IHg and MeHg resulted in different
434 metabolomes in each compartment (shoot and cytosol) with some level of coordinated regulation
435 for metabolites between shoots and cytosol. Metabolomic confirmed previous hypothesis of distinct
436 toxicity pathway for IHg and MeHg based on transcriptomics, proteomics and physiology (Larras et
437 al., 2013; Regier et al., 2013a; Beauvais-Fluck et al., 2018a). In contrast to previous proteomics and
438 transcriptomics data, Cd showed a higher impact on individual metabolites, while MeHg impacted
439 more metabolic pathways in shoots, but IHg showed a higher impact in cytosol than MeHg. New
440 omics methods are fundamentally transforming biology approaches, but the fact that many genes
441 and proteins identified by transcriptomics and proteomics have an unknown function results in
442 considerable uncertainty in the analysis of responses. Metabolomics give the opportunity to confirm
443 and reveal effects of toxicants in a complementary way to other omics methods, as it identified early
444 responses that were effective in revealing metal uptake and impact as well as were congruent with
445 expected adverse outcome pathways.

446

447 ACKNOWLEDGMENT

448 Experiments were performed at Geneva University during CC previous position. Authors thank

449 Rebecca Beauvais-Fluck, Floriane Larras, Beatriz Lobo, Nicole Regier and Debora Tanaami for their
450 help in the management of cultures, sampling of water and the preparation of cytosol extracts.

451

452 **FUNDINGS**

453 The Swiss National Science Foundation (contracts n°205321_138254 and 200020_157173).

454

455 **REFERENCES**

456 Azimi, S., Rocher, V., 2016. Influence of the water quality improvement on fish population in the
457 Seine River (Paris, France) over the 1990-2013 period. *Sci Total Environ* 542, 955-964.

458 Bailey, N.J., Oven, M., Holmes, E., Nicholson, J.K., Zenk, M.H., 2003. Metabolomic analysis of the
459 consequences of cadmium exposure in *Silene cucubalus* cell cultures via ¹H NMR spectroscopy and
460 chemometrics. *Phytochemistry* 62, 851-858.

461 Banerjee, R., Chen, S., Dare, K., Gilreath, M., Praetorius-Ibba, M., Raina, M., Reynolds, N.M., Rogers,
462 T., Roy, H., Yadavalli, S.S., Ibba, M., 2011. tRNAs: Cellular barcodes for amino acids. *FEBS Letters* 584,
463 387-395.

464 Beauvais-Fluck, R., Chaumot, A., Gimbert, F., Queau, H., Geffard, O., Slaveykova, V.I., Cosio, C., 2016.
465 Role of cellular compartmentalization in the trophic transfer of mercury species in a freshwater
466 plant-crustacean food chain. *Journal of Hazardous Materials* 320, 401-407.

467 Beauvais-Fluck, R., Gimbert, F., Mehault, O., Cosio, C., 2017. Trophic fate of inorganic and methyl-
468 mercury in a macrophyte-chironomid food chain. *Journal of Hazardous Materials* 338, 140-147.

469 Beauvais-Fluck, R., Slaveykova, V.I., Cosio, C., 2018a. Effects of two-hour exposure to environmental
470 and high concentrations of methylmercury on the transcriptome of the macrophyte *Elodea nuttallii*.
471 *Aquat Toxicol* 194, 103-111.

472 Beauvais-Fluck, R., Slaveykova, V.I., Skyllberg, U., Cosio, C., 2018b. Molecular effects, speciation and
473 competition of inorganic and methyl mercury in the aquatic plant *Elodea nuttallii*. *Environmental*
474 *Science & Technology* 52, 8876–8884.

475 Bonanno, G., Lo Giudice, R., 2010. Heavy metal bioaccumulation by the organs of *Phragmites*
476 *australis* (common reed) and their potential use as contamination indicators. *Ecological Indicators*
477 10, 639-645.

478 Bravo, A.G., Loizeau, J.L., Bouchet, S., Richard, A., Rubin, J.F., Ungureanu, V.G., Amouroux, D.,
479 Dominik, J., 2010. Mercury human exposure through fish consumption in a reservoir contaminated
480 by a chlor-alkali plant: Babeni reservoir (Romania). *Environmental Science and Pollution Research*
481 17, 1422-1432.

- 482 Castro, R., Pereira, S., Lima, A., Corticeiro, S., Valega, M., Pereira, E., Duarte, A., Figueira, E., 2009.
483 Accumulation, distribution and cellular partitioning of mercury in several halophytes of a
484 contaminated salt marsh. *Chemosphere* 76, 1348-1355.
- 485 Chambers, P.A., Lacoul, P., Murphy, K.J., Thomaz, S.M., 2008. Global diversity of aquatic
486 macrophytes in freshwater. *Hydrobiologia* 595, 9-26.
- 487 Cosio, C., Dunand, C., 2010. Transcriptome analysis of various flower and silique development stages
488 indicates a set of class III peroxidase genes potentially involved in pod shattering in *Arabidopsis*
489 *thaliana*. *Bmc Genomics* 11, 16.
- 490 Cosio, C., Fluck, R., Regier, N., Slaveykova, V.I., 2014. Effects of macrophytes on the fate of mercury
491 in aquatic systems. *Environmental Toxicology and Chemistry* 24.
- 492 Croteau, M.-N., Luoma, S.N., Stewart, A.R., 2005. Trophic transfer of metals along freshwater food
493 webs: Evidence of cadmium biomagnification in nature. *Limnology and Oceanography* 50, 1511-
494 1519.
- 495 Fraser, C.M., Chapple, C., 2011. The phenylpropanoid pathway in *Arabidopsis*. *The Arabidopsis Book*
496 / American Society of Plant Biologists 9, e0152.
- 497 Hayat, S., Hayat, Q., Alyemeni, M.N., Wani, A.S., Pichtel, J., Ahmad, A., 2012. Role of proline under
498 changing environments: A review. *Plant Signaling & Behavior* 7, 1456-1466.
- 499 Holcik, M., Sonenberg, N., 2005. Translational control in stress and apoptosis. *Nature Reviews*
500 *Molecular Cell Biology* 6, 318.
- 501 Joshi, V., Joung, J.-G., Fei, Z., Jander, G., 2010. Interdependence of threonine, methionine and
502 isoleucine metabolism in plants: accumulation and transcriptional regulation under abiotic stress.
503 *Amino Acids* 39, 933-947.
- 504 Khodayari, S., Moharramipour, S., Larvor, V., Hidalgo, K., Renault, D., 2013. Deciphering the
505 metabolic changes associated with diapause syndrome and cold acclimation in the two-spotted
506 spider mite *Tetranychus urticae*. *Plos one* 8, e54025-e54025.
- 507 Kieffer, P., Planchon, S., Oufir, M., Ziebel, J., Dommes, J., Hoffmann, L., Hausman, J.-F., Renaut, J.,
508 2009. Combining proteomics and metabolite analyses To unravel cadmium stress-response in poplar
509 leaves. *Journal of Proteome Research* 8, 400-417.
- 510 Larras, F., Regier, N., Planchon, S., Pote, J., Renaut, J., Cosio, C., 2013. Physiological and proteomic
511 changes suggest an important role of cell walls in the high tolerance to metals of *Elodea nuttallii*.
512 *Journal of Hazardous Materials* 263, 575-583.
- 513 Lemoine, R., La Camera, S., Atanassova, R., Dedaldechamp, F., Allario, T., Pourtau, N., Bonnemain, J.-
514 L., Laloi, M., Coutos-Thevenot, P., Maurousset, L., Faucher, M., Girousse, C., Lemonnier, P., Parrilla,

- 515 J., Durand, M., 2013. Source-to-sink transport of sugar and regulation by environmental factors.
516 *Frontiers in plant science* 4.
- 517 Liu, B., Yan, H., Wang, C., Li, Q., Guédron, S., Spangenberg, J.E., Feng, X., Dominik, J., 2012. Insights
518 into low fish mercury bioaccumulation in a mercury-contaminated reservoir, Guizhou, China.
519 *Environmental Pollution* 160, 109-117.
- 520 Loizeau, J.-L., Edder, P., De Alencastro, L.F., Corvi, C., Ramseier Gentile, S., 2013. La contamination du
521 Léman par les micropolluants - Revue de 40 ans d'études. *Archives des Sciences* 66, 117-136.
- 522 Ma, L., Wang, Y., Liu, W., Liu, Z., 2014. Overexpression of an alfalfa GDP-mannose 3, 5-epimerase
523 gene enhances acid, drought and salt tolerance in transgenic *Arabidopsis* by increasing ascorbate
524 accumulation. *Biotechnology Letters* 36, 2331-2341.
- 525 Masclaux-Daubresse, C., Reisdorf-Cren, M., Pageau, K., Lelandais, M., Grandjean, O., Kronenberger,
526 J., Valadier, M.-H., Feraud, M., Jouglet, T., Suzuki, A., 2006. Glutamine synthetase-Glutamate
527 synthase pathway and glutamate dehydrogenase play distinct roles in the sink-source nitrogen cycle
528 in Tobacco. *Plant Physiology* 140, 444-456.
- 529 Miesak, B.H., Coruzzi, G.M., 2002. Molecular and physiological analysis of *Arabidopsis* mutants
530 defective in cytosolic or chloroplastic aspartate aminotransferase. *Plant Physiology* 129, 650.
- 531 Moya, J.L., Ros, R., Picazo, I., 1995. Heavy metal-hormone interactions in rice plants: Effects on
532 growth, net photosynthesis, and carbohydrate distribution. *Journal of Plant Growth Regulation* 14,
533 61.
- 534 Niane, B., Guedron, S., Moritz, R., Cosio, C., Ngom, P., Deverajan, N., Pfeifer, H., Pote, J., 2014.
535 Human exposure to mercury in artisanal small-scale gold mining areas of Kedougou region, Senegal,
536 as a function of occupational activity and fish consumption. *Environmental Science and Pollution*
537 *Research*, 1-11.
- 538 Noges, T., Luup, H., Feldmann, T., 2010. Primary production of aquatic macrophytes and their
539 epiphytes in two shallow lakes (Peipsi and Vrtsjarv) in Estonia. *Aquatic Ecology* 44, 83-92.
- 540 Obata, T., Fernie, A.R., 2012. The use of metabolomics to dissect plant responses to abiotic stresses.
541 *Cellular and Molecular Life Sciences* 69, 3225-3243.
- 542 Patrick, J., Botha, F., Birch, R., 2013. Metabolic engineering of sugars and simple sugar derivatives in
543 plants. *Plant Biotechnology Journal* 11, 142-156.
- 544 Pavlikova, D., Pavlik, M., Staszko, L., Motyka, V., Szakova, J., Tlustos, P., Balik, J., 2008. Glutamate
545 kinase as a potential biomarker of heavy metal stress in plants. *Ecotoxicol Environ Saf* 70, 223-230.
- 546 Piotrowska, A., Bajguz, A., Godlewska-Zylkiewicz, B., Zambrzycka, E., 2010. Changes in growth,
547 biochemical components, and antioxidant activity in aquatic plant *Wolffia arrhiza* (Lemnaceae)

- 548 exposed to cadmium and lead. Archives of Environmental Contamination and Toxicology 58, 594-
549 604.
- 550 Raina, M., Ibba, M., 2014. tRNAs as regulators of biological processes. Front Genet 5.
- 551 Regier, N., Baerlocher, L., Munsterkotter, M., Farinelli, L., Cosio, C., 2013a. Analysis of the *Elodea*
552 *nuttallii* transcriptome in response to mercury and cadmium pollution: development of sensitive
553 tools for rapid ecotoxicological testing. Environmental Science & Technology 47, 8825-8834.
- 554 Regier, N., Beauvais-Flück, R., Slaveykova, V.I., Cosio, C., 2016. *Elodea nuttallii* exposure to mercury
555 exposure under enhanced ultraviolet radiation: Effects on bioaccumulation, transcriptome, pigment
556 content and oxidative stress. Aquatic Toxicology 180, 218-226.
- 557 Regier, N., Larras, F., Bravo, A.G., Ungureanu, V.G., Amouroux, D., Cosio, C., 2013b. Mercury
558 bioaccumulation in the aquatic plant *Elodea nuttallii* in the field and in microcosm: accumulation in
559 shoots from the water might involve copper transporters. Chemosphere 90, 595-602.
- 560 Renault, D., Puzin, C., Foucreau, N., Bouchereau, A., Petillon, J., 2016. Chronic exposure to soil
561 salinity in terrestrial species: Does plasticity and underlying physiology differ among specialized
562 ground-dwelling spiders? Journal of Insect Physiology 90, 49-58.
- 563 Renault, H., Roussel, V., El Amrani, A., Arzel, M., Renault, D., Bouchereau, A., Deleu, C., 2010. The
564 *Arabidopsis* pop2-1mutant reveals the involvement of GABA transaminase in salt stress tolerance.
565 BMC Plant Biology 10, 20.
- 566 Rizhsky, L., Liang, H., Shuman, J., Shulaev, V., Davletova, S., Mittler, R., 2004. When defense
567 pathways collide. The response of *Arabidopsis* to a combination of drought and heat stress. Plant
568 Physiology 134, 1683-1696.
- 569 Rosa, M., Prado, C., Podazza, G., Interdonato, R., Gonzalez, J.A., Hilal, M., Prado, F.E., 2009a. Soluble
570 sugars--metabolism, sensing and abiotic stress: a complex network in the life of plants. Plant
571 Signaling & Behavior 4, 388-393.
- 572 Rosa, M., Prado, C., Podazza, G., Interdonato, R., Gonzalez, J.A., Hilal, M., Prado, F.E., 2009b. Soluble
573 sugars--metabolism, sensing and abiotic stress: a complex network in the life of plants. Plant
574 Signaling & Behavior 4, 388-393.
- 575 Samecka-Cymerman, A., Kempers, A.J., 2003. Biomonitoring of water pollution with *Elodea*
576 *canadensis*. A case study of three small Polish rivers with different levels of pollution. Water Air and
577 Soil Pollution 145, 139-153.
- 578 Stoichev, T., Martin-Doimeadios, R.C.R., Tessier, E., Amouroux, D., Donard, O.F.X., 2004.
579 Improvement of analytical performances for mercury speciation by on-line derivatization,
580 cryofocussing and atomic fluorescence spectrometry. Talanta 62, 433-438.

- 581 Tohge, T., Scossa, F., Fernie, A.R., 2015. Integrative approaches to enhance understanding of plant
582 metabolic pathway structure and regulation. *Plant Physiology* 169, 1499.
- 583 Topfer, N., Scossa, F., Fernie, A., Nikoloski, Z., 2014. Variability of metabolite levels is linked to
584 differential metabolic pathways in *Arabidopsis*'s responses to abiotic stresses. *PLOS Computational*
585 *Biology* 10, e1003656.
- 586 Tzin, V., Galili, G., 2010. The biosynthetic pathways for shikimate and aromatic amino acids in
587 *Arabidopsis thaliana*. *The arabidopsis book* 8, e0132-e0132.
- 588 Valega, M., Lima, A.I.G., Figueira, E., Pereira, E., Pardal, M.A., Duarte, A.C., 2009. Mercury
589 intracellular partitioning and chelation in a salt marsh plant, *Halimione portulacoides* (L.) Aellen:
590 Strategies underlying tolerance in environmental exposure. *Chemosphere* 74, 530-536.
- 591 Venkatesh, J., Park, S.W., 2014. Role of L-ascorbate in alleviating abiotic stresses in crop plants.
592 *Botanical Studies* 55, 38.
- 593 Vital, C.E., Giordano, A., de Almeida Soares, E., Rhys Williams, T.C., Mesquita, R.O., Vidigal, P.M.P.,
594 de Santana Lopes, A., Pacheco, T.G., Rogalski, M., de Oliveira Ramos, H.J., Loureiro, M.E., 2017. An
595 integrative overview of the molecular and physiological responses of sugarcane under drought
596 conditions. *Plant Molecular Biology* 94, 577-594.
- 597 Wetzal, R.G., 2001. *Limnology – lake and river ecosystems* (3rd edition). Academic Press, San Diego.
- 598 Xu, J., Sun, J., Du, L., Liu, X., 2012. Comparative transcriptome analysis of cadmium responses in
599 *Solanum nigrum* and *Solanum torvum*. *New Phytologist* 196, 110-124.
- 600 Yancey, P.H., 2005. Organic osmolytes as compatible, metabolic and counteracting cytoprotectants
601 in high osmolarity and other stresses. *Journal of Experimental Biology* 208, 2819.
- 602 Zemanova, V., Pavlik, M., Pavlikova, D., 2017. Cadmium toxicity induced contrasting patterns of
603 concentrations of free sarcosine, specific amino acids and selected microelements in two *Noccaea*
604 species. *Plos one* 12, e0177963.
- 605 Zhang, Z., Mao, C., Shi, Z., Kou, X., 2017. The amino acid metabolic and carbohydrate metabolic
606 pathway play important roles during salt-stress response in Tomato. *Frontiers in plant science* 8,
607 1231-1231.
- 608
- 609

610

611 **Table 1.** Lignin content, chlorophyll content, performance index of PSII [PI(abs)], class III peroxidase
 612 [POD] and superoxide dismutase [SOD] activities and bioaccumulation in shoots of *Elodea nuttallii*
 613 exposed to 280 $\mu\text{g}\cdot\text{L}^{-1}$ Cd, 70 $\text{ng}\cdot\text{L}^{-1}$ IHg, or 30 $\text{ng}\cdot\text{L}^{-1}$ MeHg or not (control). For each treatment, three
 614 replicates were analyzed. Data are presented as mean \pm standard deviation (SD; n= 3). Bold font = p-
 615 value <0.05 relative to control plants.

	Shoots					Bioaccumulation		
	Lignin content ($\mu\text{g}\cdot\text{mg}^{-1}$ fresh mass)	Chlorophyll	PI (abs)	POD ($\text{nkat}\cdot\text{mg}^{-1}$ protein)	SOD ($\text{units}\cdot\mu\text{g}^{-1}$ protein)	IHg	MeHg ($\mu\text{g}\cdot\text{g}^{-1}$ dry mass)	Cd
Control	7.2 \pm 1.3	0.90 \pm 0.27	0.79 \pm 0.02	18.4 \pm 1.63	0.93 \pm 0.08	0.03 \pm 0.03	0.01 \pm 0.01	0.82 \pm 0.12
Cd	6.4 \pm 1.4	0.78 \pm 0.30	0.80 \pm 0.01	28.5 \pm 5.6	1.04 \pm 0.06	NA	NA	921 \pm 28
IHg	5.6 \pm 1.3	0.75 \pm 0.16	0.79 \pm 0.02	17.0 \pm 1.4	1.08 \pm 0.05	0.97 \pm 0.11	0.01 \pm 0.01	NA
MeHg	5.6 \pm 2.2	0.88 \pm 0.23	0.80 \pm 0.01	18.3 \pm 6.03	1.01 \pm 0.08	0.14 \pm 0.03	0.67 \pm 0.11	NA

616 NA (not analyzed).

617

618

619 **Table 2.** Concentration (nmoles·mg⁻¹ dry mass) of amino acids, organic acids, polyols and sugars
 620 (n=3; mean ± SD) whose levels significantly varied in shoots of *E. nuttallii* exposed for 24h to Cd, IHg
 621 and MeHg (bold font = p-value <0.05), relative to control plants.

	Control	Cd	IHg	MeHg
Ammonium	4.21 ± 1.03	6.12 ± 2.35	3.90 ± 0.89	7.72 ± 2.06
Aspartic Acid	15.22 ± 2.79	0.72 ± 0.84	13.41 ± 2.44	21.77 ± 1.77
BABA	0.02 ± 0.01	0.09 ± 0.06	0.07 ± 0.05	0.08 ± 0.06
Glutamine	9.03 ± 2.06	6.73 ± 1.61	8.87 ± 2.13	14.61 ± 4.43
Glycine	1.20 ± 0.20	1.00 ± 1.43	0.97 ± 0.23	1.96 ± 0.30
Histidine	0.38 ± 0.12	1.36 ± 0.45	0.30 ± 0.07	0.47 ± 0.19
Hydroxyproline	0.00 ± 0.00	0.04 ± 0.04	0.01 ± 0.01	0.02 ± 0.01
Isoleucine	0.24 ± 0.17	3.73 ± 1.14	0.15 ± 0.12	0.40 ± 0.24
Leucine	0.17 ± 0.08	2.74 ± 0.70	0.12 ± 0.05	0.28 ± 0.08
Lysine	0.25 ± 0.21	1.22 ± 0.42	0.18 ± 0.18	0.41 ± 0.34
Methionine	0.03 ± 0.01	0.04 ± 0.01	0.03 ± 0.01	0.06 ± 0.01
Methylcysteine	0.10 ± 0.05	0.03 ± 0.03	0.07 ± 0.03	0.11 ± 0.04
Phenylalanine	0.38 ± 0.08	2.15 ± 0.78	0.34 ± 0.03	0.66 ± 0.15
Proline	0.39 ± 0.15	1.93 ± 0.46	0.30 ± 0.13	0.64 ± 0.23
Serine	4.49 ± 1.05	4.64 ± 0.56	4.29 ± 1.03	7.21 ± 1.02
Threonine	1.91 ± 0.37	5.68 ± 1.72	1.73 ± 0.35	3.08 ± 0.47
Tryptophan	0.10 ± 0.02	1.60 ± 0.33	0.12 ± 0.05	0.21 ± 0.03
Tyrosine	0.14 ± 0.04	1.54 ± 0.38	0.12 ± 0.03	0.24 ± 0.03
Valine	0.52 ± 0.28	5.24 ± 1.44	0.37 ± 0.24	0.82 ± 0.41
Adonitol	0.45 ± 0.09	1.07 ± 0.31	0.46 ± 0.07	0.44 ± 0.08
Arabinose	0.65 ± 0.20	0.95 ± 0.19	0.59 ± 0.09	0.47 ± 0.07
Arabitol	0.28 ± 0.04	0.23 ± 0.04	0.18 ± 0.04	0.15 ± 0.03
Pipecolic Acid	0.65 ± 0.20	0.95 ± 0.19	0.59 ± 0.09	0.47 ± 0.08
Ribose	2.81 ± 1.02	5.43 ± 1.39	3.02 ± 0.74	3.46 ± 1.19

622

623

624

625 **Table 3.** Concentration (nmoles·mg⁻¹ dry mass) of amino acids, organic acids, polyols and sugars
 626 (n=3; mean ± SD) whose amounts significantly varied (relative to control) in the cytosol of *E. nuttallii*
 627 exposed for 24h to Cd, IHg and MeHg (bold font = p-value <0.05).

	Control	Cd	IHg	MeHg
Alpha-alanine	0.48 ± 0.01	0.31 ± 0.05	0.50 ± 0.17	0.33 ± 0.18
Ammonium	0.52 ± 0.13	0.89 ± 0.11	0.81 ± 0.07	0.62 ± 0.32
Arginine	0.16 ± 0.02	0.05 ± 0.06	0.02 ± 0.01	0.04 ± 0.04
Aspartic Acid	1.22 ± 0.12	0.60 ± 0.11	1.23 ± 0.41	0.77 ± 0.44
Glycine	0.18 ± 0.03	0.40 ± 0.03	0.12 ± 0.03	0.19 ± 0.15
Histidine	0.14 ± 0.01	0.58 ± 0.99	0.07 ± 0.01	0.0 ± 0.0
Hydroxyproline	3.68 ± 0.25	5.89 ± 0.84	4.42 ± 0.83	3.84 ± 2.01
Galactose	0.99 ± 0.01	0.39 ± 0.03	0.63 ± 0.21	0.35 ± 0.17
Mannose	0.08 ± 0.01	0.02 ± 0.01	0.04 ± 0.02	0.03 ± 0.01
Phosphoric acid	6.89 ± 1.26	15.20 ± 3.09	7.31 ± 0.82	7.26 ± 3.35

628

629

630

631

632

633

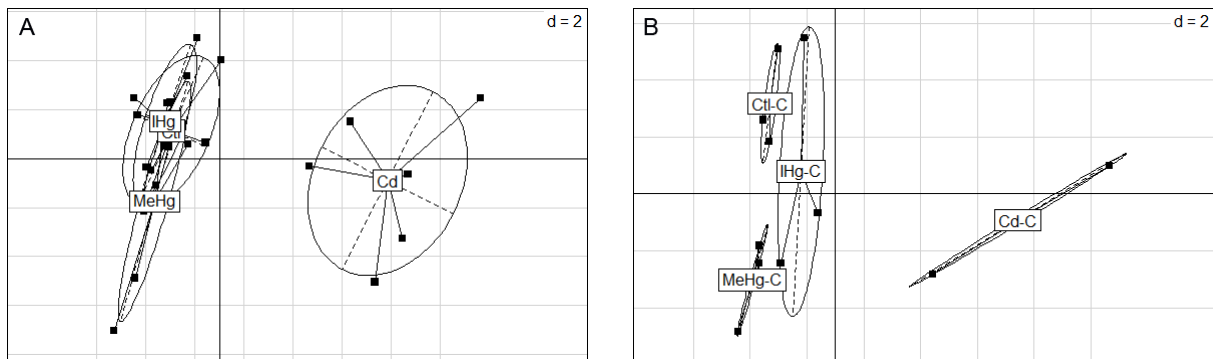


Figure 1. Principal component analysis of amino acids, organic acids, sugars and polyols measured in shoots (A) and cytosol (B) of *E. nuttallii* exposed 24h to $281 \mu\text{g}\cdot\text{L}^{-1}$ Cd, $70 \text{ ng}\cdot\text{L}^{-1}$ IHg and $30 \text{ ng}\cdot\text{L}^{-1}$ MeHg, and their control (ctl) ($n=6$ and $3 \pm \text{SD}$, respectively). PCA were calculated and plotted with the package ade4 (<http://pbil.univ-lyon1.fr/ade4>) in the R software (<http://www.r-project.org>).

634

- Cd, IHg and MeHg effects were compared in shoots and cytosol by metabolomics
- In shoots, Cd showed higher regulation, but MeHg regulated more pathways
- In cytosol, Cd had the higher impact, IHg had low effect and MeHg had very low effect
- MeHg impacts N homeostasis, and Cd results in an osmotic stress-like pattern
- Metabolomics support different molecular toxicity pathways for the three metals

Journal Pre-proof

Authors declare no conflict of interest

Journal Pre-proof